ELSEVIER

Contents lists available at ScienceDirect

Applied Ocean Research

journal homepage: www.elsevier.com/locate/apor



Research paper

The performance of bow foils in irregular and oblique waves

J.A. Bowker[©], N.C. Townsend[©]*

Faculty of Engineering and Physical Sciences, University of Southampton, UK



ARTICLE INFO

Keywords:
Wave energy
Ship propulsion
Wave augmented propulsion
Bow foils
Oblique waves

ABSTRACT

Bow foils are an emerging energy saving device that utilise wave energy to improve the efficiency of ships operating in waves, through both a reduction in ship motions and the generation of additional thrust. To identify the performance of bow foils in oblique waves, this paper presents and compares experimental results from a series of free-running model tests, with and without a bow foil, with constant forward speed, in regular and irregular oblique waves. The experiments identify the effect of bow foils on the ship heave and pitch motions, shaft torque and revolutions and foil forces and motion, over a range of relative wave headings. The results, demonstrating the ITTC QNM method, show that the bow foil reduces the delivered power required to maintain a given speed in waves, and are effective across a range of heading angles, modal periods, and wave height once a threshold is reached. The results also verify the use of spectral approaches to predict the performance of bow foils in irregular waves using transfer functions and identify that the greatest power savings are achieved in head wave conditions. The presented results provide a holistic design methodology to predict and scale the performance of bow foils across a range of sea states.

1. Introduction

With increasingly stringent ship regulations (IMO, 2022), national targets (Maritime, 2019), the development of energy saving technologies which exploit the ambient renewable energy are receiving significant attention. For example photovoltaic (PV) energy systems to supplement auxiliary hotel loads have been trialled on various ships (Lee et al., 2012; World's, 2011; Yuan et al., 2018; Atkinson, 2016; D'Orazio, 2013) and wind-augmented propulsion systems e.g. Flettner rotors, sails and kites (Wellicome, 1975; Lu and Ringsberg, 2020; Chou et al., 2021; Nelissen et al., 2016; Traut et al., 2014) are widely reported with commercial prototypes and systems under development (Smart, 2025; Econowind, 2025). Wave augmented propulsion using bow foils is an emerging technology to improve ship efficiency in waves. Bow foils exploit wave energy through both a reduction in ship heave and pitch motions and the generation of additional thrust, to reduce the delivered power required to maintain a given speed in waves, saving fuel and reducing emissions (Mei et al., 2023; Bowker and Townsend, 2022a,b; Bockmann, 2015; Filippas et al., 2020).

Table 1 summarises investigations into the effect of bow foils on ship motions and propulsive efficiency. The research, following initial investigations by Jakobsen (1981) and Naito et al. (1986), has primarily focused on: numerical prediction (Belibassakis and Filippas, 2015; Belibassakis and Politis, 2013; De Silva and Yamaguchi, 2012; Bockmann and Steen, 2016a; Isshiki et al., 1984), foil pitch mechanism (Bockmann

and Steen, 2014; Naito and Isshiki, 2005), foil size and location (Feng et al., 2014; Naito and Isshiki, 2005), ship coupling (Bowker et al., 2020; Filippas, 2015; Feng et al., 2014), resistance and propulsion (Belibassakis et al., 2021a; Feng et al., 2014), free surface effects (Filippas et al., 2020), trim-pitch stabilisation (Ntouras et al., 2022), emission reductions (Belibassakis et al., 2021a; Bockmann et al., 2018; Huang et al., 2016; Isshiki, 2015) and incorporation into the IMO energy efficiency framework (Feng et al., 2014; Rozhdestvensky and Htet, 2021; Bowker et al., 2023; Bockmann and Steen, 2016a). In addition, full scale sea trials have previously been conducted on a 15.7 m fishing vessel (Terao and Isshiki, 1991), a 20 m trawler (M.N et al., 1995) and 25.4 m trawler (Dybdahl, 1988) and recently commercially for ferries (Yrke and Bockmann, 2019; WaveFoil, 2025).

The studies show heave motion reductions (between 10% and 33%), pitch reductions (between 11% and 28%) and a significant reduction in ship added resistance (up to 80%) (Niklas and Pruszko, 2023; Bowker and Townsend, 2022b; Bockmann and Steen, 2016b; Feng et al., 2014). A key performance parameter is the wave phasing parameter, the phase difference between the relative bow foil motions and the wave orbital velocity (De Silva and Yamaguchi, 2012; Bowker and Townsend, 2022b). A 90° wave phasing is considered optimal, whereby the relative bow foil motion coincides (and opposes) the wave orbital velocity, resulting in a greater flow velocity over the flapping foil, and maximum foil forces i.e., thrust. The wave phasing parameter is related to the

E-mail addresses: J.Bowker@soton.ac.uk (J.A. Bowker), nick@soton.ac.uk (N.C. Townsend).

^{*} Corresponding author.

Table 1
Bow foil research articles.
Source: Reproduced from Bowker and Townsend (2023).

Research article	Ship type	Ship length (m)	Speed (knots)	Froude number (Fn)	Wave type	Wavelength/Ship length $(\lambda/L)^a$
Model tests						
Isshiki and Murakami (1983)	-	80	Varies ^c	Varies ^c	Regular	0.78-4.88
Konstantinov and Yakimov	-	125	7 ^c	0.10	Regular	1.60
(1995) ^b						
Naito et al. (2001) ^b	Container ship	175	16.1	0.20	Regular	0.50-2.00
					& Irregular	0.22-1.07
Naito (2003) ^b	Container ship	175	22.9	0.284	Regular	1.50
Feng et al. (2014) ^b	Container ship	175	22.0	0.275	Regular	0.50-3.20
Bockmann (2015) ^b	Platform supply vessel	80.8	12.0	0.22	Regular	0.82-2.55
Huang et al. (2016)	Container ship	168.8	16.6	0.21	Regular	1.00, 1.30
Bockmann and Steen (2016b) ^b	Tanker	113.2	11,13	0.17, 0.20	Regular	0.68-2.33
					& Irregular	0.84–2.68
Chikarenko (2019)	-	105	Varies ^c	Varies ^c	Regular	1.35-3.52
Belibassakis et al. (2021b) ^b	Ferry	107	17	0.25	Regular	0.84-1.56
Bowker and Townsend (2022b)	Bulk carrier	100	11	0.18	Regular	0.86–1.85
Ntouras et al. (2022) ^b	Ferry	107	16–11	0.176-0.25	Regular	0.87-1.62
Numerical simulations						
Grue et al. (1988)	_	40	8	0.21	Regular	2.5
Naito and Isshiki (2005)	Container ship	175	16.1	0.20	Irregular	0.59
Chiu et al. (2014)	Tanker	315	12-16.5	0.11-0.15	Regular	1
Belibassakis and Filippas	Series 60	50	10.7	0.25	Regular	0–4
(2015)	hullform		10.7	0.20	regum	· .
(2010)					& Irregular	0.91-2.25
Isshiki (2015)	Bulk carrier	178	15.6	0.19	Irregular	0.39-1.16
Rozhdestvensky and Htet	Container	175	16,20	0.20,0.25	Regular	0.82-2.55
(2021)			., .			
Belibassakis et al. (2021a)	Bulk carrier	109	14	0.22	Irregular	1.09
, , ,	and Ferry	107	17	0.265	Irregular	1.07
Zhang et al. (2022)	Container ship	175	5	0.06	Regular	1
Zilding Ct di. (2022)					& Irregular	0.72
Mei et al. (2023)	Naval combatant	142	4.9-20.3	0.067-0.28	Regular	1.70
Full scale trials						
Berg (1985)	Yacht	7.5	6 ^c	0.36	Actual seas	_
beig (1900)					(Oslo,	
					Norway)	
Dybdahl (1988)	Trawler	20	6	0.22	Actual seas	4
,,,			-	*	(Trondheim,	•
					Norway)	
Terao and Isshiki (1991)	Trawler	15.7	7.4	0.31	Actual seas	0.93
Tetao and Issinki (1991)	Trawici	10.7	7.1	0.01	(Miho &	0.55
					Kunou,	
					Japan)	
M NI at al. (100E)	Trawler	25.4	10.1	0.33	Actual seas	1.86
M.N et al. (1995)	Hawlei	23.4	10.1	0.33		1.00
					(Baltic,	
Velco and Bookmann (2010)	Form	40	10 E	0.27	Russia)	
Yrke and Bockmann (2019)	Ferry	40	10.5	0.27	Actual seas	_
					(Faroe	
					Islands,	
0					Denmark)	
Specific ship routes	0 1:		10.1	0.00		v 4 p 12
Isshiki et al. (1984)	Cargo ship	80	12.1	0.22	Irregular	North Pacific
Veritec (1985)	-	20,40,70	10.9,15.9	0.21-0.31	Irregular	North Sea
Veritec (1986)	-	180	17	0.22	Irregular	North Atlantic
Feng et al. (2014)	Container ship	214.2	22.5	0.25	Irregular	North Pacific
Bockmann et al. (2018)	Cargo ship	99.9	12–16	0.20-0.26	Irregular	North Sea & Bay of Bisc
Bowker and Townsend	Bulk carrier	75–150	9.5-13.4	0.18	Irregular	North Sea, North Atlanti
(2022a)						M
(2022a)						North Pacific &

^a Wavelength based on mean wave period.

length of the wave relative to the ship's length (i.e., the wavelength to ship length ratio). Multiple studies report optimal wavelength to ship length ratios (in head waves) of around 1–1.3 (Konstantinov and Yakimov, 1995; Naito and Isshiki, 2005; Feng et al., 2014; Bockmann

and Steen, 2016b; Belibassakis et al., 2021b; Bowker and Townsend, 2022b). Based on optimal wavelength to ship length ratios a global assessment of bow foil ship lengths is given in Bowker and Townsend (2023). The results suggest that for most regions (e.g., North Atlantic,

^b Also include equivalent numerical simulations.

^c Solely propelled by waves.

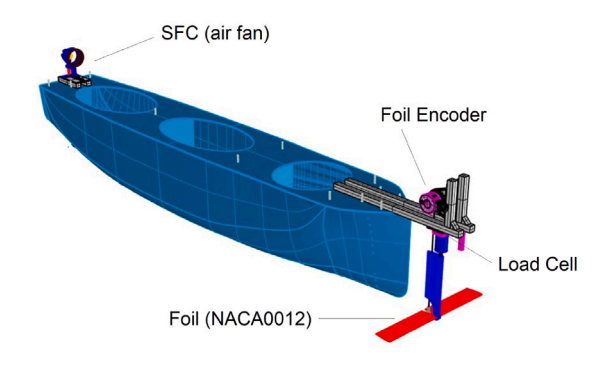




Fig. 1. CAD image and photograph of the model.

North Pacific and North Sea regions) a ship length of around 145 m (and a maximum of up to approximately 220 m) is favourable for installation of bow foils, although subject to local variations. While in the Mediterranean ship lengths less than 100 m may be more favourable. Interestingly, the completed full scale trials are significantly smaller than the types of ships investigated at model scale and in numerical simulations.

Currently, there are limited studies that have considered the effect of oblique waves on the performance of bow foils. Prediction methodologies in oblique waves have been developed by Feng et al. (2014), Belibassakis et al. (2021b) and Bowker and Townsend (2022a). In Bowker and Townsend (2022a) a methodology to predict the performance of a passive bow foil in irregular, short crested (oblique waves) over various routes is presented, building on direct measurement of the delivered power from model scale, free running experiments over a range of wave frequencies in head sea conditions. Similarly, Feng et al. (2014) presents a coupled hull-foil numerical model, verified against experiments in head waves, to predict the performance using spectral approaches in irregular waves, for a fixed foil system. While Belibassakis et al. (2021b) considers an actively controlled foil system, based on a boundary element method (BEM), presenting results for head (180 degrees) and quartering seas (150 degrees), for 1 irregular wave case $(H_s/L = 0.03, T_pU/L = 0.7)$, with comparison to regular head wave experiments. That is, all methods either verify or extrapolate from (regular) head wave experiments. To date no experimental studies have considered the effect of oblique waves on the performance and verified these approaches. With reportedly large variations depending on ship heading and encountered sea state from the predictions (Bowker and

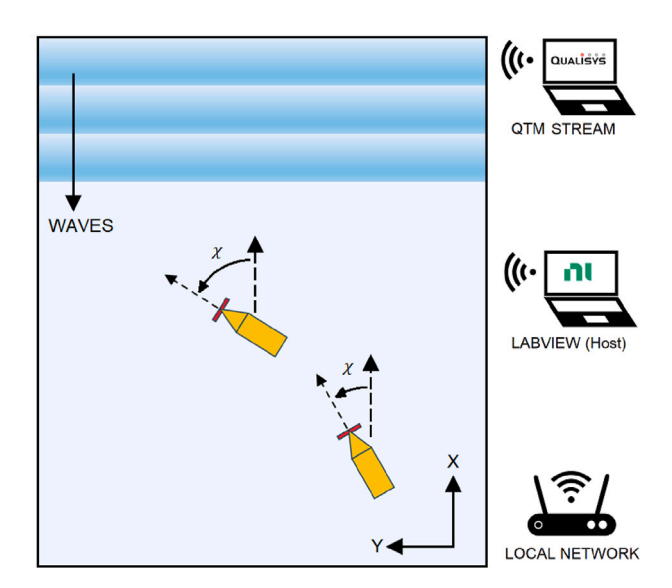


Fig. 2. Schematic of the experimental setup.

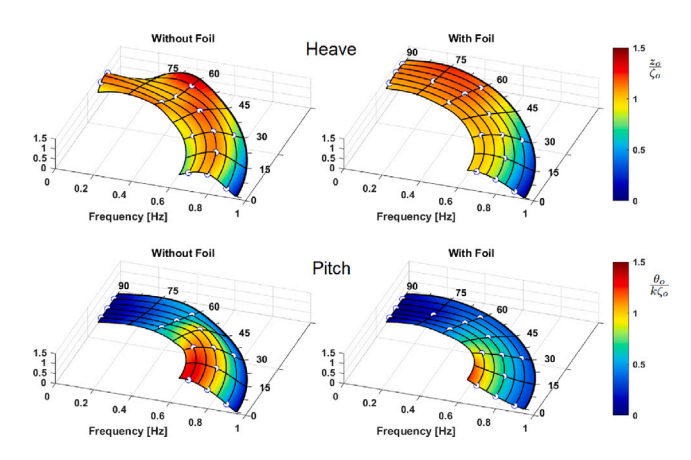


Fig. 3. Heave and pitch response amplitude operators (RAOs), with and without the bow foil over a range of heading angles ($\zeta_o = 0.02 \text{ m}, V_m = 0.8 \text{ m/s}$) (Curve fit using a Modified Akima Interpolation).

Townsend, 2022a) (with the percentage foil retraction a significant factor in operational deployment) establishing the performance of bow foils in oblique waves is important for evaluation of this technology.

1.1. Paper contribution and outline

This paper presents and compares experimental results from a series of free-running model tests, with and without a passive bow foil, with constant forward speed, in regular and irregular oblique waves. The results, which compare (regular) transfer functions to irregular spectrum responses, identify the effect of oblique waves on the performance. In addition to, demonstrating a methodology to assess bow foil technology and verifying the ITTC QNM method for predicting delivered power from model tests.

The paper outline is as follows: Section 2 presents the experimental methodology and experimental setup. The results, including the regular and then irregular ship motions, propeller torque and rpm, and foil responses are presented in Section 3. A discussion, including the scaling considerations and full scale predictions are presented in Section 4 demonstrating the potential of this emerging technology.

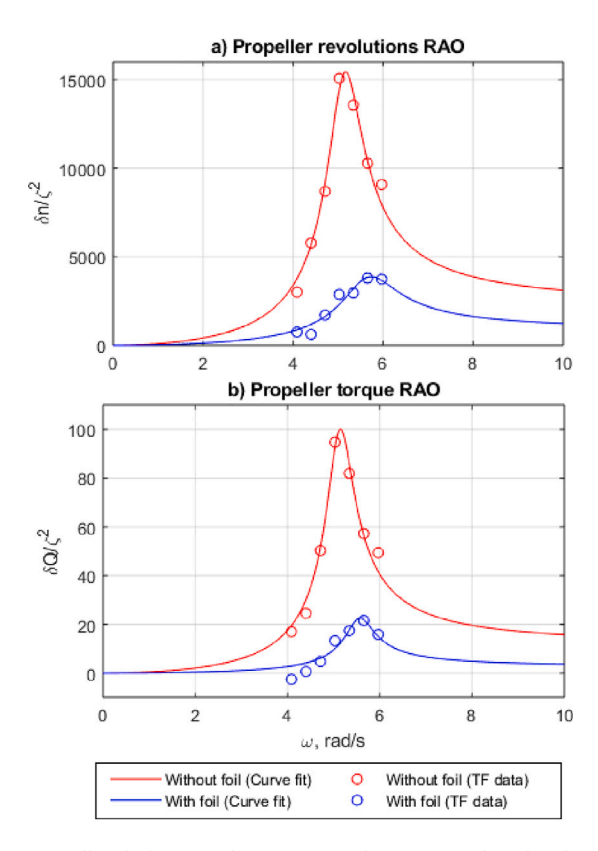


Fig. 4. Propeller shaft rpm and torque in regular waves, with and without the bow foil ($\chi=0^\circ,\zeta_o=0.02$ m, $V_m=0.8$ m/s).

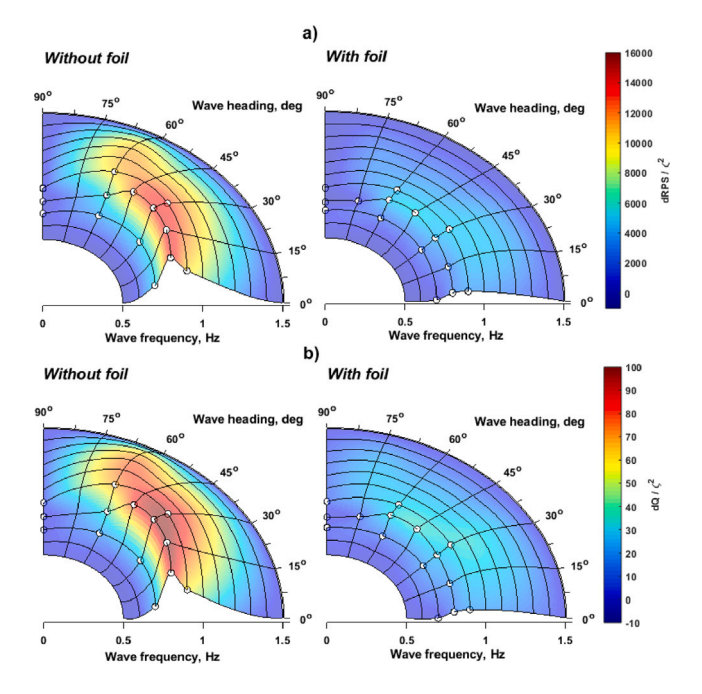


Fig. 5. Propeller shaft rpm and torque in regular waves, over a range of headings, with and without the bow foil ($\zeta_o=0.02~{\rm m},V_m=0.8~{\rm m/s}$) (Curve fit using a Modified Akima Interpolation).

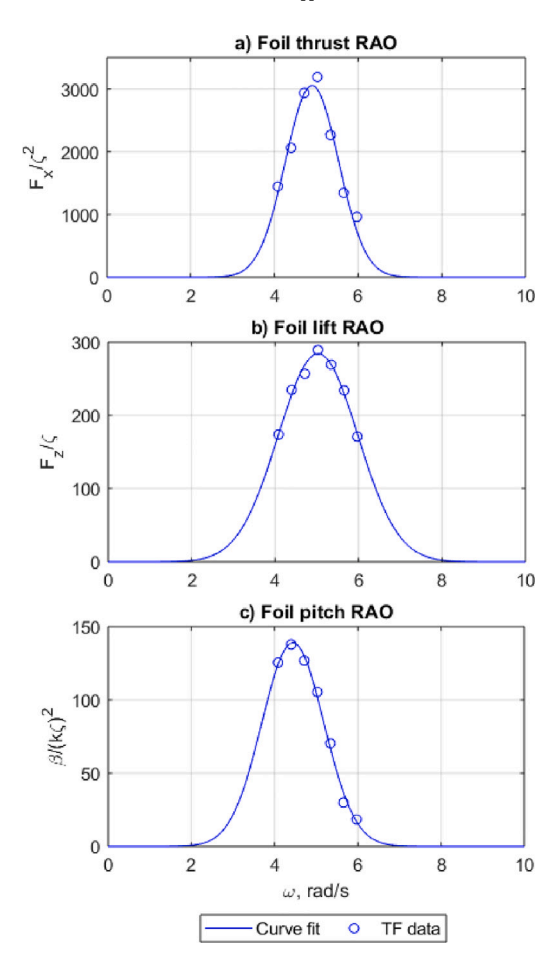


Fig. 6. Foil thrust, lift and pitch angles in regular waves ($\chi=0^{\circ},\zeta_{o}=0.02~{\rm m},V_{m}=0.8~{\rm m/s}$).

2. Methodology

2.1. Overview

To identify the performance of bow foils in oblique waves, a series of free-running model tests, with and without a passive, spring-loaded bow foil, over a range of wave frequencies, in regular and irregular oblique waves with constant forward speed, were conducted in the Haslar Ocean Basin (Length = 120 m, Width = 60 m, Depth = 5 m). The model, a 1:50 scale small bulk carrier, is shown in Fig. 1. The model and foil properties are summarised in Table 2. Details of the model are also presented in Bowker and Townsend (2022b) and Lamont et al. (2023).

2.2. Experimental setup

Fig. 2 shows a schematic of the experimental setup. The data acquisition (DAQ) and control system was based on a National Instruments myRIO1900 and LabVIEW software. The model heading and forward speed were controlled in real time based on the streamed 6DOF motions of the model from a motion tracking camera system (Qualisys). A proportional-derivative (PD) feedback controller was used to maintain the model heading in the Ocean Basin, by controlling the rudder angle. While a proportional–integral (PI) feedback controller was used to control the propeller rpm and forward speed of the model.

Details of the data acquisition, control and sensors are given in Table 3. The data was recorded at a sample rate of 100 Hz. The waves were recorded using 9 different wave probes situated around the test

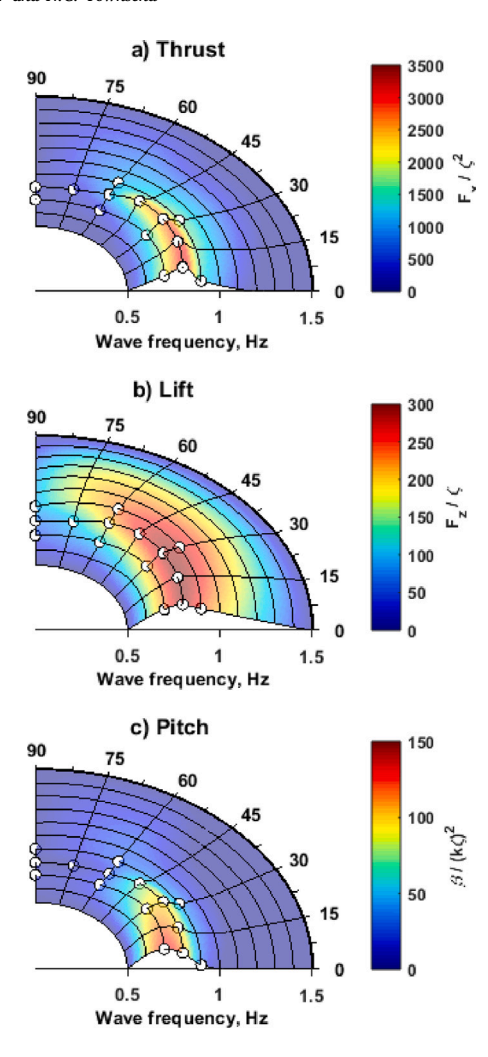


Fig. 7. Foil thrust, lift and pitch angles in regular waves over a range of headings ($\zeta_o=0.02~{\rm m},V_m=0.8~{\rm m/s}$) (Curve fit using a Modified Akima Interpolation).

Table 2
Model hullform and foil properties.

Value
1:50
2
0.33
0.12
51.50
0.65
0.65
NACA0012
NACA0012
NACA0012 60
NACA0012 60 420
NACA0012 60 420 7
NACA0012 60 420 7 0.165

facility. The load cell and torquemeter were calibrated following the National Physics Laboratory (NPL) guidelines (Robinson, 2008).

To provide the skin friction correction (SFC), a ducted air fan was mounted to the stern via a load cell, as shown in Fig. 1. The required SFC load was calculated from the difference between the model and full-scale skin friction coefficient (i.e. $\Delta C_f = C_{fm} - C_{fs}$) using the ITTC '57 frictional correlation line based on the respective Reynolds Number for the model and ship speeds (ITTC, 1957).

Table 3Sensor information.

Sensor	Type	Range
Shaft torquemeter	Full bridge	0-0.1 N m
Shaft encoder (rpm)	Optical	2500 ppr
Tri-axial load cell	Half bridge	±10 N
Foil pitch encoder	Optical	2048 ppr
SFC Load cell	Full bridge	±5 N
Rudder potentiomenter	Resistance	±50 deg
Motion capture (Qualisys)	Optical	-
Wave probes (facility)	Ultrasonic	-

Table 4
Experimental investigations.

Parameter	Value		
Ship model speed (V_m) [m/s]	0.8		
Froude number (V/\sqrt{gL})	0.18		
Regular waves			
Wave amplitude (ζ_o) [m]	0.02		
Wave frequencies (ω_o) [Hz]	0.65, 0.70, 0.75, 0.80, 0.85, 0.90, 0.95		
Ship heading (χ) [deg]	0° (head), 15°, 30°, 45°, 60°, 90° (beam)		
Irregular waves			
Significant wave heights (H _s) [m]	0.02, 0.04, 0.06, 0.08, 0.1		
Model wave periods (T_0) [s]	0.95, 1.10, 1.25, 1.36, 1.62, 1.85		
Ship heading (χ) [deg]	0° (head), 15°, 30°, 45°, 60°, 90° (beam)		

2.3. Experimental investigations

The experimental investigations are summarised in Table 4. Following the ITTC guidelines, over 10 (steady state) wave encounters at each heading in regular waves were captured. In irregular waves, where 100 encounters are preferable, two irregular wave runs (of different timedomain realisations or 'seeds') were conducted to acquire sufficient encounters to accumulate the spectral responses.

The experimental procedure, which for the regular wave tests followed the procedure in Bowker and Townsend (2022b), comprised of a zero speed datum, followed by an initial acceleration in calm water, before encountering waves and settling into a steady state response (with a controlled average model speed of 0.8 m/s and at least 10 wave encounters recorded), before switching to a new heading and reaching steady state (for at least 10 wave encounters). While the irregular wave tests comprised of a single heading in each test. To summarise, the data was processed as:

- Synchronisation. The Qualisys and DAQ data sets were synchronised to the same time base.
- Crop. The data was cropped into a datum at the start of the run and steady state responses (comprising of at least 10 wave encounters for each regular wave headings).
- Filter. The data was filtered using a Butterworth low-pass filter, with cutoff frequencies of: 1 Hz for shaft rpm, 2 Hz for the torquemeter and 5 Hz for the motions and foil forces.
- Analyse. Sine wave fitting was used to identify the amplitude, phase and encounter frequencies.

3. Results

3.1. Regular waves

3.1.1. Motions

Fig. 3 shows the heave and pitch response amplitude operators (RAOs), with and without the bow foil, over the range of investigated heading angles. The results show that the effect of the bow foil reduces the heave and pitch motions in oblique head wave conditions (χ : 0° to 45°). While, in oblique beam wave conditions (χ : 45° to 90°) the effect

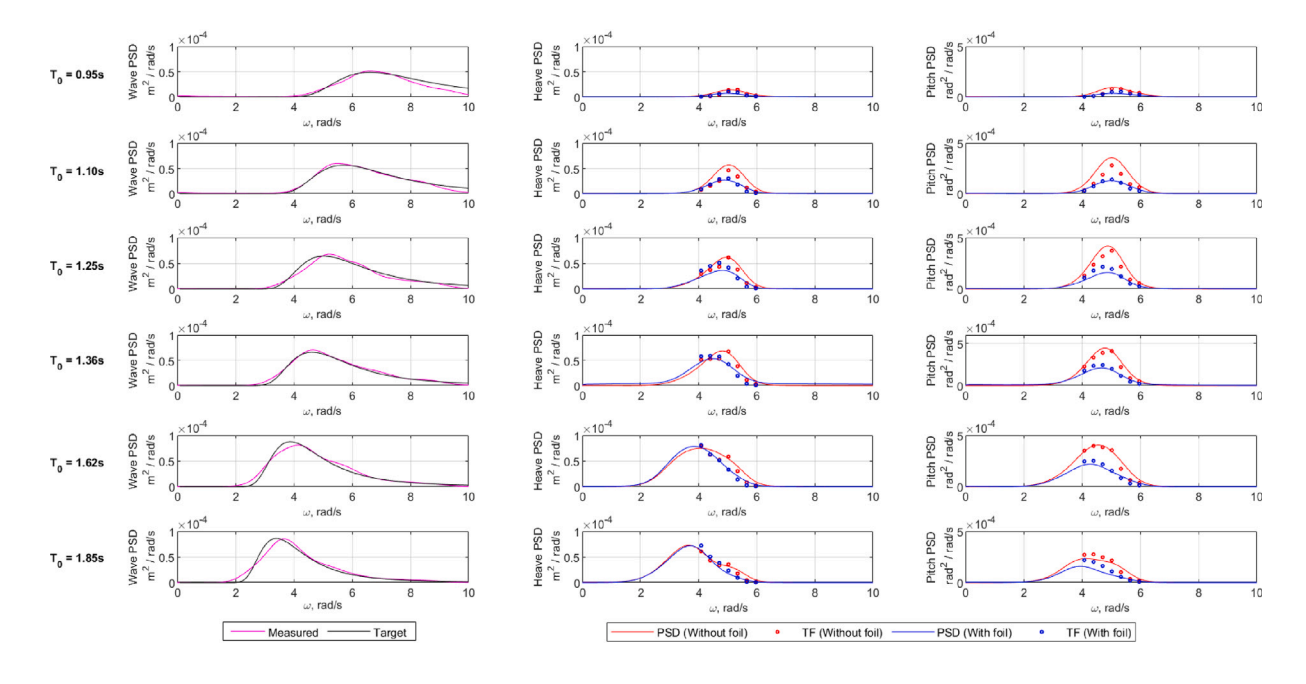


Fig. 8. Comparison of irregular and regular response spectra ($\chi = 0^{\circ}, H_s = 0.06 \text{ m}, V_m = 0.8 \text{ m/s}$).

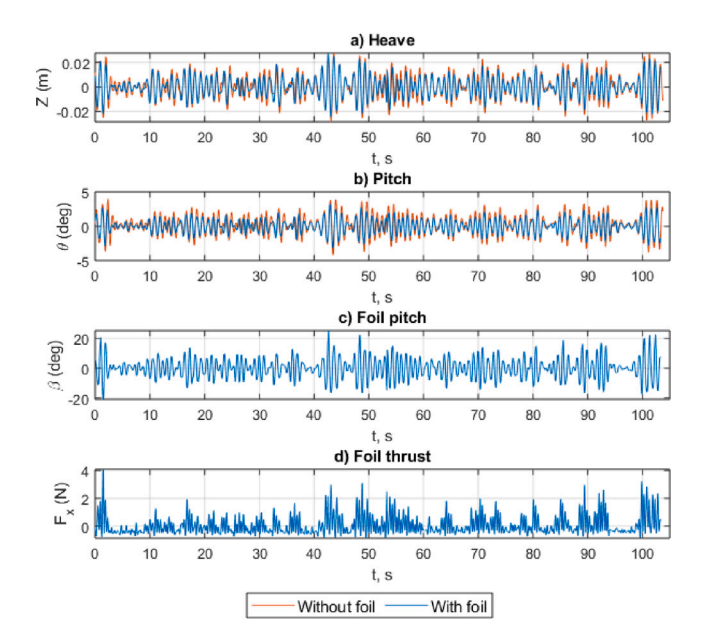


Fig. 9. Example irregular heave and pitch responses with and without the bow foil and foil pitch and thrust ($\chi=0^{\circ}, H_s=0.06 \text{ m}, T_0=1.25 \text{ s}, V_m=0.8 \text{ m/s}$).

of the foil leads to a heave contouring motion and the pitch motion, with and without a foil, is negligible. That is, the results show that the bow foil is advantageous in reducing the heave and pitch motions in oblique head wave conditions.

3.1.2. Shaft torque and revolutions

Fig. 4 shows the propeller shaft rpm and torque in regular head waves ($\chi=0^{\circ}$), with and without the bow foil. The bow foil leads to a reduction in rpm and torque required to maintain a given speed in waves, as expected and shown in previous work (Bowker and Townsend, 2022b). Eq. (1) was used to approximate the relationship and provide a transfer function of the torque and rpm over the

frequency range.

$$f(\omega) = \frac{\omega^2}{\sqrt{(c - a\omega^2)^2 + (b^2\omega^2)}}$$
 (1)

Extending over the range of investigated regular wave headings, Fig. 5, shows the propeller rpm and torque with and without the bow foil. The results show a general reduction with heading angle (through head $\chi=0^\circ$ to beam waves $\chi=90^\circ$) and that the bow foil reduces the rpm and torque, particularly around resonance from 0° through to $\approx 60^\circ$. That is, the bow foil savings are more pronounced in head wave conditions.

3.1.3. Foil thrust, lift and pitch angles

Fig. 6 shows the foil thrust, lift and pitch angles in regular head waves ($\chi=0^{\circ}$), with and without the bow foil (with a $\frac{1}{\sqrt{2\pi\sigma^2}}e^{-\frac{(x-\mu)^2}{2\sigma^2}}$ curve fit). In this study the hydrodynamic lift and thrust forces are defined in the ship fixed axis frame. These results show that the thrust and lift forces occur at similar (resonance) frequencies, although the maximum foil pitch response occurs at a slightly lower frequency.

The foil responses over the range of heading angles, Fig. 7, are more pronounced in head wave conditions. This is attributed to both the relatively greater flapping motion of the foil in head waves and the optimum alignment with the incoming wavy flow. Interestingly, the thrust and pitch responses of the foil tail off after $\chi \approx 45^{\circ}$, although the lift forces remain for heading angles up to 60°. This may indicate the foil damping and reduction of added resistance is associated with the vertical (lift) forces and that the additional thrust, which is greatest in head waves when the foil is aligned to the incoming waves, is related to when the foil flapping motion is exhibited.

3.2. Irregular waves

Fig. 9 shows an example time history of the irregular wave responses with and without the bow foil. By starting the model at the same time under 'autonomous' control and maintaining the irregular wave seeding, the model encountered the same 'wave train' enabling this direct comparison to be made.

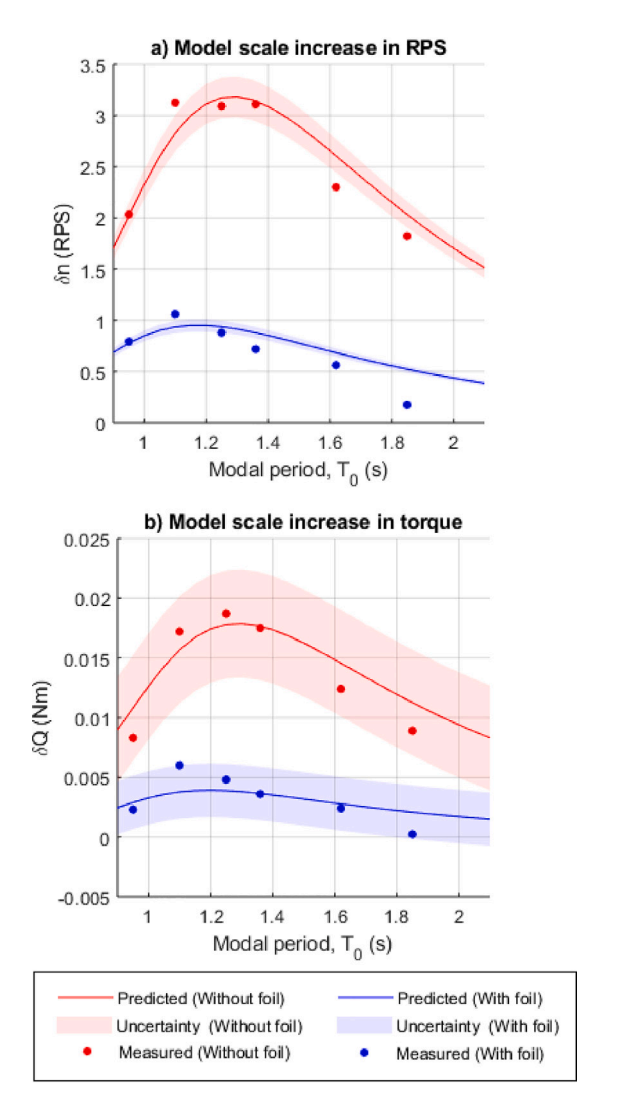


Fig. 10. Effect of modal period (T_0) on the shaft rpm and torque with and without the bow foil, in irregular waves compared to irregular response estimated from regular responses.

3.2.1. Modal period

Fig. 8 shows the irregular wave and motion response spectra. The results show that the generated waves closely represent the target wave spectra and that the regular and irregular motions show close agreement across the investigated modal periods. The results also indicate that the bow foil reduces the heave and pitch motions, for the investigated cases.

Comparing the rpm and torque (to maintain a constant speed in waves), Fig. 10, the bow foil leads to a reduction across the investigated modal periods. That is, for the investigated sea states the bow foil performance is largely advantageous. Although, extrapolating the results the bow foil may need to be retracted in sea states with lower and higher modal periods.

3.2.2. Wave height

The effect of significant wave height is shown in Figs. 11–13. Fig. 11 illustrates the irregular heave time histories, over a range of significant wave heights, with the same seeding. The spectral responses, Fig. 12, show that the generated waves closely represent the targeted spectra. Fig. 13 shows that the required rpm and torque to maintain a given speed, increases with wave height, and the irregular results show close agreement and similar trends with the transfer functions for both with

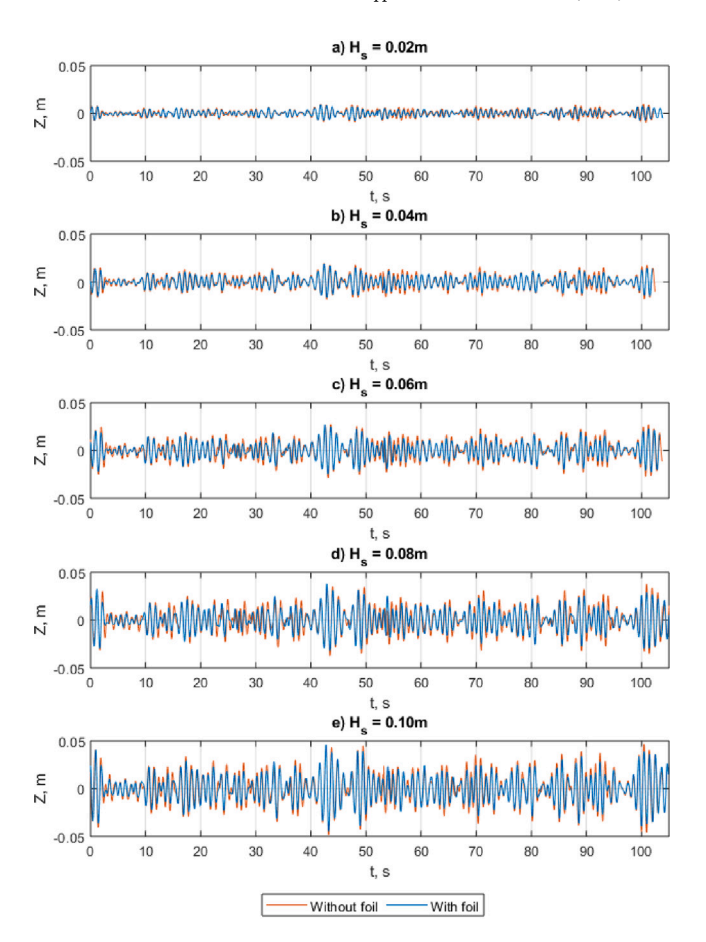


Fig. 11. Example irregular experiments with increasing significant wave height, with and without the bow foil ($\chi=0^{\circ},T_0=1.25$ s, $V_m=0.8$ m/s).

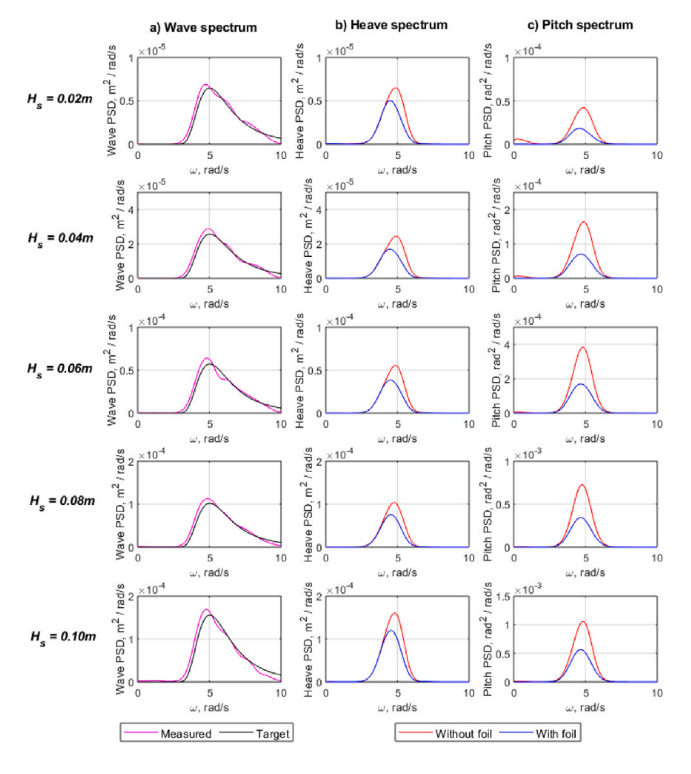


Fig. 12. Comparison of wave, heave and pitch spectra with increasing significant wave height, with and without the bow foil ($\chi = 0^{\circ}, T_0 = 1.25 \text{ s}, V_m = 0.8 \text{ m/s}$).

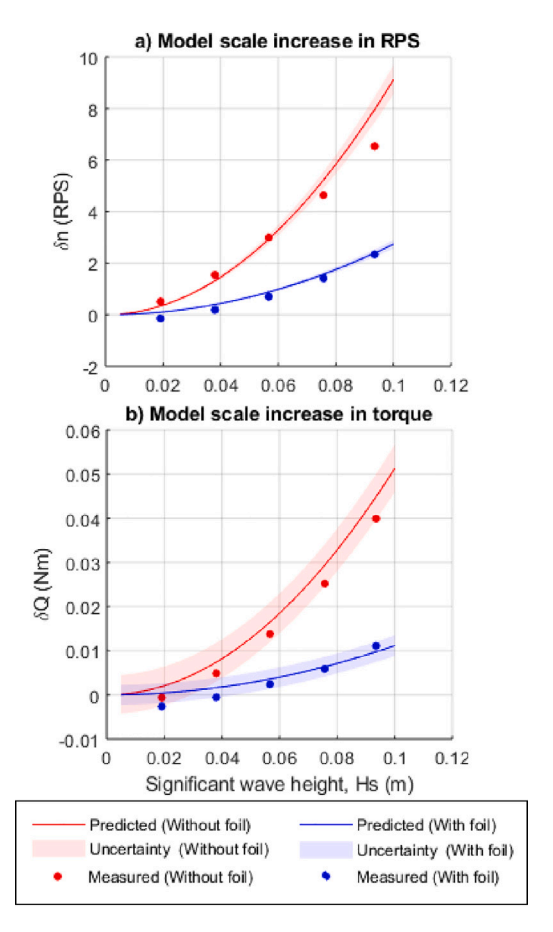


Fig. 13. Effect of significant wave height (H_s) on the shaft rpm and torque with and without the bow foil, in irregular waves compared to irregular response estimated from regular responses.

and without the bow foil. The experiments show that the bow foil performance increases with wave height, indicating that foil stall did not occur. Although, with further increases in the wave height the foil would be expected to stall, requiring a change in foil stiffness or retraction of the foils in practice.

3.3. Relative wave heading

The effect of the relative wave heading is shown in Fig. 14. The results show that the bow foil reduces the rpm and torque, required to maintain a given speed in waves, effective across a range of heading angles up to $\chi \approx 60^{\circ}$.

4. Discussion

4.1. Full scale delivered power

Fig. 15 shows the predicted change in delivered power (δP_d) for the nominal full scale vessel (L=100 m), and the effects of modal period, significant wave height and heading in regular and irregular waves on the performance. The predicted change in delivered power, calculated as:

$$\delta P_{b,f} = 2\pi \left[(Q_{sw} + \delta Q_{b,f})(n_{sw} + \delta n_{b,f}) - Q_{sw} n_{sw} \right] \tag{2}$$

and the efficiency:

$$\eta = \frac{\delta P_b - \delta P_f}{P_{sw} + \delta P_b} \tag{3}$$

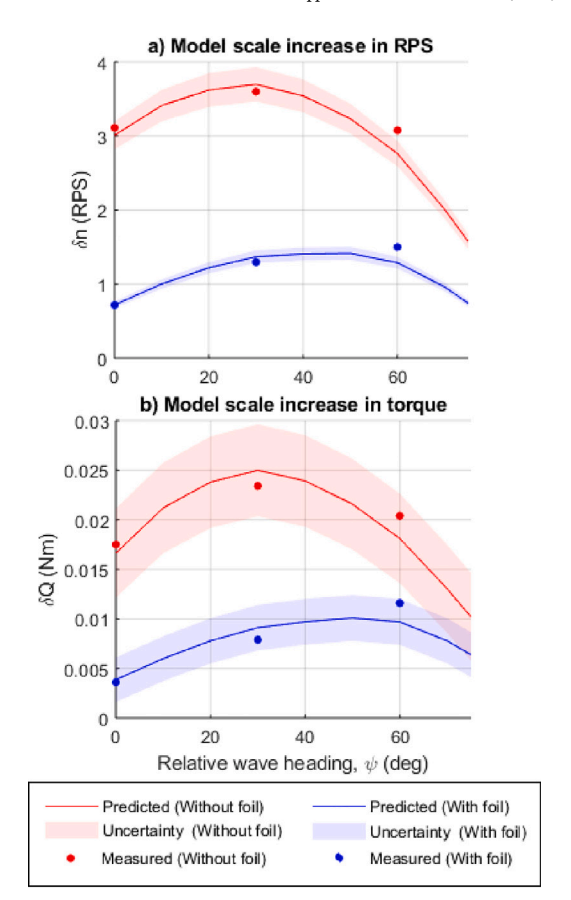


Fig. 14. Effect of relative wave heading (χ) on the shaft rpm and torque with and without the bow foil, in irregular waves compared to irregular response estimated from regular responses.

where Q, n represents the shaft torque and rps respectively and $\delta P_f, \delta P_h$ represents the change in delivered power with and without the foil and P_{sw} represents the calm water delivered power. The subscripts b, f refer to the bare hull or the hull with the foil and sw the still water (calm water) condition. The results shows that the bow foil is advantageous in relative head wave conditions, for a range of modal periods around resonance and wave heights once a threshold is reached. Interestingly, the effect of heading angle shows that the efficiency is greater encountering waves at a slight heading angle (not directly head on) for the investigated sea states. This finding is attributed to the change in effective encounter wavelength (i.e., $\lambda_e/L \approx 1$). However, the magnitude of the delivered power reduction remains greatest encountering head waves. This result suggests that performance gains may be possible by 'wave' routing, to maximise head waves. In practice, these results indicate that bow foils should be retractable, deployed to reduce the added resistance (or speed loss) in relative head waves.

4.2. Full scale foil forces

Extending the methodology to the foil, Fig. 16, the irregular thrust and lift forces determined from the regular transfer functions, and measured irregular responses can be scaled to provide a prediction of the full scale ship performance. These results show that predicting the performance from regular wave responses can provide reasonable estimates of the irregular responses. The results show that the forces and flapping motion of the foil generally reduce with relative heading angle, increase with wave height and the thrust and pitching of the foil are frequency dependent. Although, the predicted lift forces using regular spectral approaches under predict compared to the scaled irregular responses. This finding suggests the vertical forces are greater

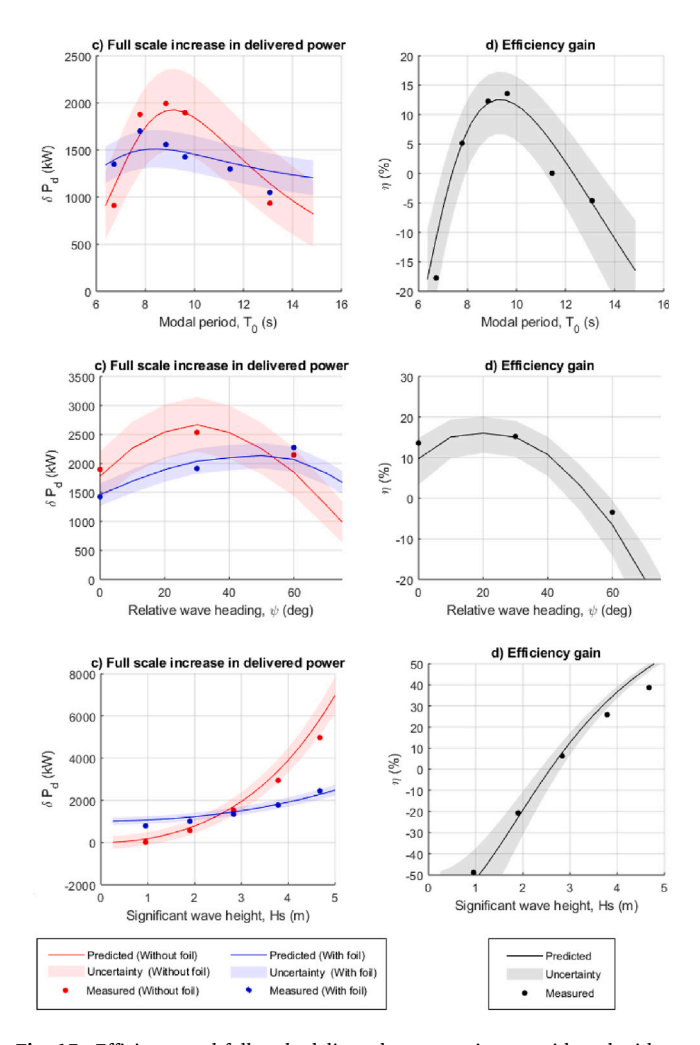


Fig. 15. Efficiency and full scale delivered power estimates with and without the bow foil in irregular oblique waves ((a) Effect of modal period (b) Effect of significant wave height (c) Effect of relative wave heading).

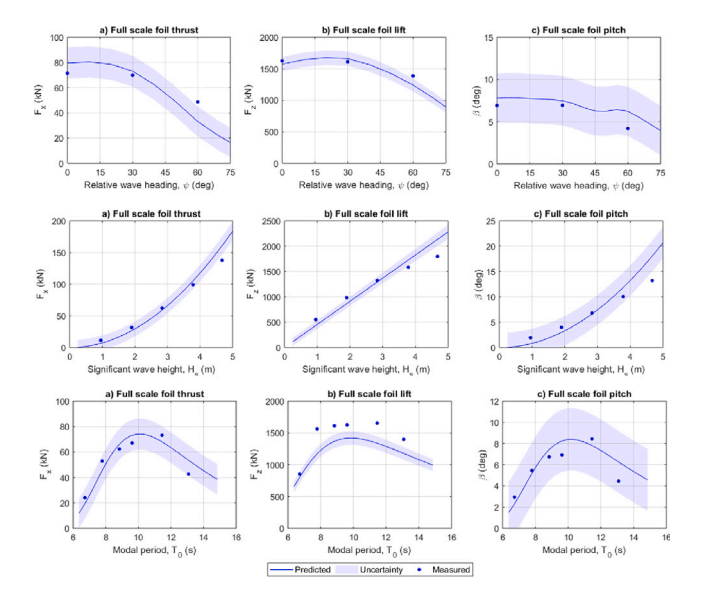


Fig. 16. Full Scale estimates of foil thrust, lift and pitch in irregular oblique waves ((a) Effect of modal period (b) Effect of significant wave height (c) Effect of relative wave heading).

in irregular waves than the regular responses may imply, and safety factors should be selected carefully.

5. Conclusion

This paper presented results from a series of free-running, model scale experiments, identifying the performance of a passive, spring loaded, bow foil in regular and irregular, long crested, oblique waves. The results, comparing the performance with and without the bow foil, shows a reduction in ship heave and pitch motions and the delivered power (required to maintain a given speed in waves) is effective across a range of heading angles up to $\chi \approx 60^{\circ}$. Performance savings increase with wave height once a threshold is reached and with modal periods around resonance (i.e. where $\lambda_e/L \approx 1$). Practically, these findings suggest that a change in foil stiffness or retraction of the bow foil would be required in sea states with low or high modal periods and small wave heights. Furthermore, the presented results demonstrate the ITTC QNM method and verify the use of spectral approaches to predict the performance of bow foils in irregular waves from transfer functions including the foil forces. The results and method provide a holistic design methodology to predict and scale the performance of bow foils across a range of sea states.

CRediT authorship contribution statement

J.A. Bowker: Writing – review & editing, Visualization, Methodology, Investigation, Formal analysis, Data curation. **N.C. Townsend:** Writing – review & editing, Writing – original draft, Supervision, Project administration, Methodology, Investigation, Funding acquisition, Conceptualization.

Declaration of competing interest

The authors declare the following financial interests/personal relationships which may be considered as potential competing interests: Nicholas Townsend reports financial support was provided by European Union. If there are other authors, they declare that they have no known competing financial interests or personal relationships that could have appeared to influence the work reported in this paper.

Acknowledgement

This research was supported by the EU as part of the SeaTech project (https://seatech2020.eu/).



This project has received funding from the European Union's Horizon 2020 research and innovation programme under grant agreement No 857840

The opinions expressed in this document reflect only the author's view and in no way reflect the European Commission's opinions. The European Commission is not responsible for any use that may be made of the information it contains.

References

Atkinson, G.M., 2016. Analysis of marine solar power trials on blue star delos. J. Mar. Eng. Technol. 15 (3), 115–123. http://dx.doi.org/10.1080/20464177.2016. 1246907.

Belibassakis, K., Bleuanus, S., Vermeiden, J., Townsend, N., 2021a. Combined performance of innovative biomimetic ship propulsion system in waves with dual fuel ship engine and application to short-sea shipping. In: The 31st International Ocean and Polar Engineering Conference.

- Belibassakis, K.A., Filippas, E.S., 2015. Ship propulsion in waves by actively controlled flapping foils. Appl. Ocean Res. 52, 1–11. http://dx.doi.org/10. 1016/j.apor.2015.04.009, URL https://www.sciencedirect.com/science/article/pii/ S0141118715000541.
- Belibassakis, K.A., Filippas, E.S., Papadakis, G., 2021b. Numerical and experimental investigation of the performance of dynamic wing for augmenting ship propulsion in head and quartering seas. J. Mar. Sci. Eng. 10.
- Belibassakis, K.A., Politis, G.K., 2013. Hydrodynamic performance of flapping wings for augmenting ship propulsion in waves. Ocean Eng. 72, 227–240. http://dx.doi.org/10.1016/j.oceaneng.2013.06.028, URL https://www.sciencedirect.com/science/article/pii/S0029801813002746.
- Berg, A., 1985. Trials with passive foil propulsion on M/S Kystfangst. Trondheim. Techn. Rep. Proj. 672.
- Bockmann, E., 2015. Wave Propulsion of Ships (Ph.D. thesis).
- Bockmann, E., Steen, S., 2014. Experiments with actively pitch-controlled and spring-loaded oscillating foils. Appl. Ocean Res. 48, 227–235. http://dx.doi.org/10.1016/j.apor.2014.09.004, URL https://www.sciencedirect.com/science/article/pii/S0141118714000923
- Bockmann, E., Steen, S., 2016a. Calculation of EEDIweather for a general cargo vessel.

 Ocean Eng. 122, 68–73. http://dx.doi.org/10.1016/j.oceaneng.2016.06.007, URL https://www.sciencedirect.com/science/article/pii/S0029801816301871.
- Bockmann, E., Steen, S., 2016b. Model test and simulation of a ship with wavefoils.

 Appl. Ocean Res. 57, 8–18. http://dx.doi.org/10.1016/j.apor.2016.02.002, URL https://www.sciencedirect.com/science/article/pii/S0141118716300244.
- Bockmann, E., Yrke, A., Steen, S., 2018. Fuel savings for a general cargo ship employing retractable bow foils. Appl. Ocean Res. 76, 1–10. http://dx.doi.org/10. 1016/j.apor.2018.03.015, URL https://www.sciencedirect.com/science/article/pii/S0141118717304091.
- Bowker, J.A., Tan, M., Townsend, N.C., 2020. Forward speed prediction of a free-running wave-propelled boat. IEEE J. Ocean. Eng. 46 (2), 402–413.
- Bowker, J., Townsend, N., 2022a. A probabilistic method to evaluate bow foils for realistic seas and shipping routes. Appl. Ocean Res. 129, 103374.
- Bowker, J.A., Townsend, N.C., 2022b. Evaluation of bow foils on ship delivered power in waves using model tests. Appl. Ocean Res. 123, 103148. http://dx.doi.org/10. 1016/j.apor.2022.103148, URL https://www.sciencedirect.com/science/article/pii/ S0141118722000079
- Bowker, J., Townsend, N., 2023. The effect of ship length scale on bow foil efficiency gains in waves. In: OCEANS 2023-Limerick. IEEE, pp. 1–10.
- Bowker, J., Townsend, N., Bulten, N., Bleuanus, S., 2023. Comparison of ship energy efficiency methods for bow foil technology. In: OCEANS 2023-Limerick. IEEE, pp. 1–9.
- Chikarenko, V., 2019. Arrangement of wave propulsors on a ship. Mosc. Univ. Mech. Bull. 74 (2), 41–43.
- Chiu, F.-C., Li, W.-F., Tiao, W.-C., 2014. Preliminary study on a concept of wave propulsion by an active pitch-oscillating fin. In: OCEANS 2014 - TAIPEI. pp. 1–5. http://dx.doi.org/10.1109/OCEANS-TAIPEI.2014.6964558.
- Chou, T., Kosmas, V., Acciaro, M., Renken, K., 2021. A comeback of wind power in shipping: An economic and operational review on the wind-assisted ship propulsion technology. Sustainability 13 (4), 1880.
- De Silva, L.W.A., Yamaguchi, H., 2012. Numerical study on active wave devouring propulsion. J. Mar. Sci. Technol. 17 (3), 261–275. http://dx.doi.org/10.1007/s00773-012-0169-y.
- 2013. An inside look at the world's largest solar powered boat, The verge [online]. URL https://www.theverge.com/2013/6/22/4454980/ms-turanor-planetsolar-solar-powered-boat-photo-essay.
- Dybdahl, K., 1988. Foilpropellen kan revolusjonere skipsfarten. Tek. Ukeblad Tek. 39, 10–11.
- 2025. Econowind. https://econowind.nl/.
- Feng, P., Ma, N., Gu, X., 2014. A practical method for predicting the propulsive performance of energy efficient ship with wave devouring hydrofoils at actual seas. Proc. Inst. Mech. Eng. Part M: J. Eng. Marit. Environ. 228 (4), 348–361. http: //dx.doi.org/10.1177/1475090213489674, URL https://journals.sagepub.com/doi/ abs/10.1177/1475090213489674.
- Filippas, E.S., 2015. Augmenting ship propulsion in waves using flapping foils initially designed for roll stabilization. Procedia Comput. Sci. 66, 103–111. http://dx.doi.org/10.1016/j.procs.2015.11.013, URL https://www.sciencedirect.com/science/article/pii/S1877050915033621.
- Filippas, E.S., Papadakis, G.P., Belibassakis, K.A., 2020. Free-surface effects on the performance of flapping-foil thruster for augmenting ship propulsion in waves. J. Mar. Sci. Eng. 8 (5), 357, URL https://www.mdpi.com/2077-1312/8/5/357.
- Grue, J., Mo, A., Palm, E., 1988. Propulsion of a foil moving in water waves. J. Fluid Mech. 186, 393–417. http://dx.doi.org/10.1017/S0022112088000205, URL https://www.cambridge.org/core/article/propulsion-of-a-foil-moving-in-water-waves/DF02E53C625251EF98EC47CD06AF767D.
- Huang, S., Wu, T., Hsu, Y., Guo, J., Tsai, J., Chiu, F., 2016. Effective energy-saving device of eco-ship by using wave propulsion. In: 2016 Techno-Ocean. Techno-Ocean, pp. 566–570. http://dx.doi.org/10.1109/Techno-Ocean.2016.7890719.
- IMO, 2022. Guidelines on the Method of Calculation of the Attained Energy Efficiency Existing Ship Index (EEXI) (Resolution MEPC.350(78)). Report, International Maritime Organisation.

- Isshiki, H., 2015. Utilization of wave energy to improve propulsive and seekeeping performances of a ship in rough weather. Asian J. Eng. Technol. 03.
- Isshiki, H., Murakami, M., 1983. A theory of wave devouring propulsion (3rd report).
 An experimental verification of thrust generation by a passive-type hydrowing propulsor. J. Soc. Nav. Archit. Jpn. 154, 125–135.
- Isshiki, H., Murakami, M., Terao, Y., 1984. Utilization of wave energy into propulsion of ship-wave devouring propulsion. In: 15th Symposium on Naval Hydrodynamics. Hamburg, Germany, pp. 539–552.
- 1957. ITTC model-ship correlation line. In: In 8th International Towing Tank Conference.
- Jakobsen, E., 1981. The foil propeller, wave power for propulsion. URL https://ci.nii.ac.jp/naid/80001169029/en/.
- Konstantinov, G., Yakimov, Y., 1995. Calculation of the thrust of a wave-powered marine propelling device. Fluid Dyn. 30 (3), 453-456.
- Lamont, M., Bowker, J.A., Townsend, N.C., 2023. Data acquisition and autonomous control of free running ship models using video motion capture. In: The 7th International Conference on Advanced Model Measurement Technology for the Maritime Industry. AMT'23.
- Lee, K.J., Shin, D.S., Lee, J.P., Yoo, D.W., Choi, H.K., Kim, H.J., 2012. Hybrid photovoltaic/diesel green ship operating in standalone and grid-connected mode in South Korea Experimental investigation. In: 2012 IEEE Vehicle Power and Propulsion Conference. VPPC 2012, VPPC 2012, Vol. 49, 580–583.URL http://dx.doi.org/10.1016/j.energy.2012.11.004,
- Lu, R., Ringsberg, J.W., 2020. Ship energy performance study of three wind-assisted ship propulsion technologies including a parametric study of the flettner rotor technology. Ships Offshore Struct. 15 (3), 249–258.
- 2019. Maritime 2050 navigating the future.
- Mei, L., Yan, W., Zhou, J., Shi, W., 2023. Thrust enhancement of DTMB 5415 with elastic flapping foil in regular head waves. J. Mar. Sci. Eng. 11 (3), http://dx.doi. org/10.3390/jmse11030632, URL https://www.mdpi.com/2077-1312/11/3/632.
- M.N, A.Nikolaev., Savitsky, Senkin, Y., 1995. Basics of calculation of the effciency of a ship with propulsor of the wing type. Sudostroenie 4, 7–10.
- Naito, S., 2003. Effect of bow wings on ship propulsion. In: Proceedings of 2nd International Symposium on Aqua Bio-Mechanisms. Honolulu, US.
- Naito, S., Higaki, S., Kato, J., Mizuno, S., Yamamori, T., 2001. Reduction of added resistance and thrust generation by using bow wings in waves. J. Kansai Soc. Nav. Archit. 235, 79–89.
- Naito, S., Isshiki, H., 2005. Effect of bow wings on ship propulsion and motions. Appl. Mech. Rev. 58 (4), 253–268. http://dx.doi.org/10.1115/1.1982801.
- Naito, S., Isshiki, H., Fujimoto, K., 1986. Thrust generation of a fin attached to a ship in waves.
- Nelissen, D., Traut, M., Kohler, J., Mao, W., Faber, J., Ahdour, S., 2016. Study on the Analysis of Market Potentials and Market Barriers for Wind Propulsion Technologies for Ships. Tech. Rep. 16.7G92.114, Delft (CE Deflt).
- Niklas, K., Pruszko, H., 2023. The retrofitting of ships by applying retractable bow hydrofoils: a case study. J. Ocean. Eng. Mar. Energy 9 (4), 767–788.
- Ntouras, D., Papadakis, G., Belibassakis, K., 2022. Ship bow wings with application to trim and resistance control in calm water and in waves. J. Mar. Sci. Eng. 10 (4), 492
- Robinson, A., 2008. Guide to the Calibration and Testing of Torque Transducers. Tech. Rep. 107, National Physics Laboratory.
- Rozhdestvensky, K.V., Htet, Z.M., 2021. A mathematical model of a ship with wings propelled by waves. J. Mar. Sci. Appl..
- 2025. Smart green shipping. https://smartgreenshipping.com/.
- Terao, Y., Isshiki, H., 1991. Wave devouring propulsion sea trial. Eighteenth Symp. Nav. Hydrodyn. 287–296.
- Traut, M., Gilbert, P., Walsh, C., Bows, A., Filippone, A., Stansby, P., Wood, R., 2014.
 Propulsive power contribution of a kite and a Flettner rotor on selected shipping routes. Appl. Energy 113, 362–372. http://dx.doi.org/10.1016/j.apenergy.2013.07. 026.
- Veritec, 1985. Analysis of a Foil Propeller as an Auxiliary Propulsion System. Tech. Rep. 85–3326.
- Veritec, 1986. Analysis of a Foil Propeller as an Auxiliary Propulsion System. Tech. Rep. 86–3413.
- 2025. Wavefoil. www.wavefoil.com.
- Wellicome, J., 1975. A broad appraisal of the economic and technical requisites for a wind driven merchant vessel. In: Ship Science Reports. University of Southampton, Southampton, UK, URL https://eprints.soton.ac.uk/43217/1/003.pdf.
- 2011. World's first solar-power-assisted vessel further developed-car carrier auriga leader to be fitted with hybrid power supply system and ballast-water management system, and adapted to use low-sulfur fuel. https://global.kawasaki.com/en/corp/newsroom/news/upload_pdf/20110525_1.pdf.
- Yrke, A., Bockmann, E., 2019. Full-Scale Experience with Retractable Bow Foils on M/F Teistin. Tech. Rep., WaveFoil.
- Yuan, Y., Wang, J., Yan, X., Li, Q., Long, T., 2018. A design and experimental investigation of a large-scale solar energy/diesel generator powered hybrid ship. Energy 165, 965–978. http://dx.doi.org/10.1016/j.energy.2018.09.085.
- Zhang, Y., Xu, L., Ding, Z., Hu, M., 2022. Wave propulsion and sea-keeping enhancement for ships in rough sea condition by flapping foils. Ocean Eng. 266, 112802. http://dx.doi.org/10.1016/j.oceaneng.2022.112802.